Cell Reports
Article

Cell PRESS
Open ACCESS

BET Bromodomain Inhibition Triggers Apoptosis of NF1-Associated Malignant Peripheral Nerve Sheath Tumors through *Bim* Induction

Amish J. Patel,[1,2] Chung-Ping Liao,[1] Zhiguo Chen,[1] Chiachi Liu,[1] Yong Wang,[1] and Lu Q. Le[1,3,4,*]
[1]Department of Dermatology
[2]Cancer Biology Graduate Program
[3]Harold C. Simmons Cancer Center
[4]UTSW Neurofibromatosis Clinic
University of Texas Southwestern Medical Center at Dallas, Dallas, TX, 75390-9133, USA
*Correspondence: lu.le@utsouthwestern.edu
http://dx.doi.org/10.1016/j.celrep.2013.12.001

SUMMARY

Malignant peripheral nerve sheath tumors (MPNSTs) are highly aggressive sarcomas that develop sporadically or in neurofibromatosis type 1 (NF1) patients. There is no effective treatment for MPNSTs and they are typically fatal. To gain insights into MPNST pathogenesis, we utilized an MPNST mouse model that allowed us to study the evolution of these tumors at the transcriptome level. Strikingly, in MPNSTs we found upregulation of a chromatin regulator, Brd4, and show that BRD4 inhibition profoundly suppresses both growth and tumorigenesis. Our findings reveal roles for BET bromodomains in MPNST development and report a mechanism by which bromodomain inhibition induces apoptosis through induction of proapoptotic Bim, which may represent a paradigm shift in therapy for MPNST patients. Moreover, these findings indicate epigenetic mechanisms underlying the balance of anti- and proapoptotic molecules and that bromodomain inhibition can shift this balance in favor of cancer cell apoptosis.

INTRODUCTION

Neurofibromatosis type 1 (NF1) is one of the most common human genetic disorders of the nervous system and affects one in 3,500 individuals around the world regardless of ethnicity and gender (Wallace et al., 1990). NF1 manifests through inheritance or sporadic mutation of the *Nf1* tumor suppressor gene, a negative regulator of oncogenic p21-RAS, which predisposes NF1 patients to a wide spectrum of symptoms including developmental, neurological, dermatological, and cardiovascular defects and tumor development (Le and Parada, 2007; Martin et al., 1990). Although NF1 patients are susceptible to developing various neoplasms (juvenile myelomonocytic leukemia, optic glioma, astrocytoma, rhabdomyosarcoma), the most common occurring are benign neurofibromas, which can be stratified into two subgroups: plexiform and dermal (Albers and Gutmann, 2009; Bajenaru et al., 2003; Le and Parada, 2007; Shannon et al., 1992). Plexiform neurofibromas can progress to malignant sarcomas known as malignant peripheral nerve sheath tumors (MPNSTs), which account for 10% of all soft tissue sarcomas (King et al., 2000). They are highly aggressive, incurable through conventional chemotherapy or surgical resection, and a leading cause of mortality in the NF1 patient population (Duong et al., 2011). Although significant progress in understanding NF1 tumor development has been made, surgery remains the standard of care for MPNST patients, and prognosis remains bleak (Zou et al., 2009).

Neurofibroma progression to MPNST in NF1 patients is associated with additional genetic changes including amplification/overexpression of oncogenic receptor tyrosine kinases (i.e., EGFR, PDGFR, MET) or growth factors (i.e., neuregulin-1, hepatocyte growth factor) and loss of tumor suppressors *Ink4a*, *Pten*, or *P53* (the latter being the most common) (Cichowski et al., 1999; Endo et al., 2011; Gregorian et al., 2009; Huijbregts et al., 2003; Joseph et al., 2008; Keng et al., 2012; Ling et al., 2005; Perrone et al., 2009; Perry et al., 2002; Torres et al., 2011; Vogel et al., 1999). Modeling these genetic changes alongside loss of *Nf1* in mice has been reported to promote MPNST development, which confirms their contributions to MPNST pathogenesis. This has led to the identification of therapeutic targets regulating the cell cycle, thus allowing for inhibition of proliferation, but eventual resistance or tumor burden are likely to hinder the efficacy of such agents (Albritton et al., 2006; Jessen et al., 2013; Johannessen et al., 2008; Mo et al., 2013; Patel et al., 2012; Wu et al., 2013a). Selective inhibition of both proliferation and survival may offer MPNST patients a better prognosis. However, limited capability to culture human MPNSTs and lack of a model system that permits genome-wide analysis or functional interrogation of MPNSTs and their pre-tumorigenic counterparts have hindered the elucidation of

survival dependencies in MPNSTs. We and others have developed mouse models in which genetic loss of tumor suppressors *Nf1* and *P53* leads to spontaneous initiation of MPNSTs (Cichowski et al., 1999; Vogel et al., 1999) (L.Q.L., unpublished data). More recently, we identified skin-derived precursors (SKPs) with *Nf1* deficiency to be a cell of origin for dermal neurofibromas (Le et al., 2009).

Serendipitously, we found that *Nf1*-deficient SKPs are also capable of giving rise to plexiform neurofibromas when transplanted into a nerve, and further loss of *P53* readily allows for malignant transformation into MPNSTs with histological and molecular features consistent with human MPNSTs (Mo et al., 2013; Chau et al., 2013). This MPNST mouse model affords us the opportunity to monitor the evolution of these tumors from stem cell to benign neurofibroma to MPNST. Here, we utilized our SKP-derived MPNST model to study the evolution of these tumors by comparative transcriptome analysis of SKP-derived MPNSTs (sMPNSTs) and their pretumorigenic ancestors, *Nf1*;*P53*-deficient SKPs (NP-SKPs), and identify upregulation of *Brd4* in MPNSTs.

We investigated the role of BRD4 in MPNST pathogenesis. BRD4 is a BET (bromodomain and extraterminal) family member that contains two bromodomains in tandem, which permit recognition and binding to acetylated histones, and subsequent recruitment of cofactors (including pTEFb) for RNA polymerase-II-dependent transcription elongation (Dey et al., 2003; Jang et al., 2005; Wu et al., 2013b; Yang et al., 2005). BRD4 is reported to regulate expression of mitotic genes required for cell-cycle progression, and its fusion to NUT (nuclear protein in testis) has been implicated in the pathogenesis of NUT-midline carcinomas (Filippakopoulos et al., 2010; Mochizuki et al., 2008; Yang et al., 2008). The development of selective small molecule inhibitors of BRD4, called JQ1, I-BET 151, and CPI203, has allowed for selective inhibition of C-Myc expression and self-renewal in hematopoietic malignancies (acute myeloid leukemia, mixed lineage leukemia, multiple myeloma, and T cell acute lymphoblastic leukemia), thus establishing JQ1 or I-BET 151-mediated inhibition of BRD4 as therapeutic strategy to disable oncogenic C-Myc (Dawson et al., 2011; Delmore et al., 2011; King et al., 2013; Zuber et al., 2011). Recent evidence indicates that BRD4 and Mediator together occupy mostly active genes in multiple myeloma cells, and at high concentrations at superenhancers for key oncogenic drivers or cell identity genes (Lovén et al., 2013). These superenhancer-regulated genes have been shown to be highly sensitive to levels of BRD4 or its cofactors, such that selective inhibition with JQ1 leads to substantial suppression of their transcription elongation, whereas active genes with typical enhancers are less affected (Lovén et al., 2013). All together, these findings suggest that the concentration/levels of BRD4 and its cofactors are important for the maintaining high levels of cancer cell specific oncogenes, thus indicating a general strategy for identifying dependencies in diverse cancer types (Lovén et al., 2013). Whether the levels of BRD4 and its cofactors are important for solid tumor initiation and progression, including MPNSTs, remains unknown.

Here, we show that increased levels of BRD4 accompany the progression of pretumorigenic NP-SKPs to MPNSTs in vivo. Genetic and pharmacological inhibition of BRD4 substantially inhibits both in vitro growth and in vivo tumorigenesis of NF1-associated MPNSTs. Transcriptome and genomic occupancy analysis of BRD4 inhibition in MPNSTs reveals downregulation of *Cyclin D1* and *Bcl2* expression along with derepression of *Bim* transcription, which we demonstrate to suppress tumorigenesis and initiate apoptosis of MPNSTs. Collectively, our findings reveal a role for BET bromodomains in maintaining the growth and survival of NF1-associated MPNSTs and identify a therapeutic strategy for selective inhibition of MPNST tumorigenesis and survival, which may serve to improve the prognosis for NF1-associated MPNST patients.

RESULTS

Transcriptome Analysis of $Nf1^{-/-}$ $P53^{-/-}$ SKP Progression to MPNST Identifies Upregulation of Brd4

Previously, we established a mouse model of dermal neurofibroma (dNF) where we demonstrate that *Nf1*-deficient SKPs can give rise to dNFs, which is contingent on their local microenvironment (Le et al., 2009). In the course of these SKP and neurofibroma studies, we serendipitously found that we could faithfully generate MPNSTs from SKPs doubly deficient in *Nf1* and *P53* (NP-SKPs) (Mo et al., 2013; Chau et al., 2013). This finding creates a powerful MPNST model that affords us the opportunity to genetically monitor the evolution of MPNSTs from their pretumorigenic precursors (NP-SKPs). These SKP-derived MPNSTs (sMPNSTs) were found to have a robust potential for giving rise to tumors when either transplanted as tumor fragments or as few as 10,000 cells, whereas their ancestors (NP-SKPs) required at least 100,000 cells and longer time in vivo to become sMPNSTs. These observations led us to hypothesize that dual loss of tumor suppressors *Nf1* and *P53* is required but not sufficient for progression of NP-SKPs to sMPNSTs. We envisioned that further genetic or epigenetic changes, the microenvironment, cells of origin, or multiple factors are required for progression to MPNST. Although these complexities pose challenges to addressing our hypothesis, we reasoned that underlying transcriptome changes would allow us to molecularly understand tumor initiation, maintenance, and progression regulated in this model system. Advantageously, our MPNST mouse model allows us to take our transcriptome insights and systematically and rapidly determine how MPNST tumorigenesis is regulated. Therefore, we compared the gene expression profiles of sMPNST tumors to their pretumorigenic ancestors (NP-SKPs) via microarray analysis to understand what transcriptome changes occur after MPNST tumor initiation/progression (Figure 1A). As anticipated, comparative microarray analysis indicates that sMPNST tumors had numerous genes up- and downregulated when compared to their ancestors (NP-SKPs). However, we found substantially more genes upregulated, and with greater magnitude of fold change expression (Figure 1B), which was associated with upregulation of RNA polymerase II (RNAP II) regulator *Brd4* (Figure 1C). Quantitative RT-PCR and western blot analyses confirm these findings (Figures 1D and 1E). Consistent with these data, we also observed abundant expression of BRD4 in human MPNST primary tissue and xenograft (Figure S1). BRD4 along with Mediator and pTEFb are all implicated in promoting RNA polymerase-II (RNAP II)-dependent

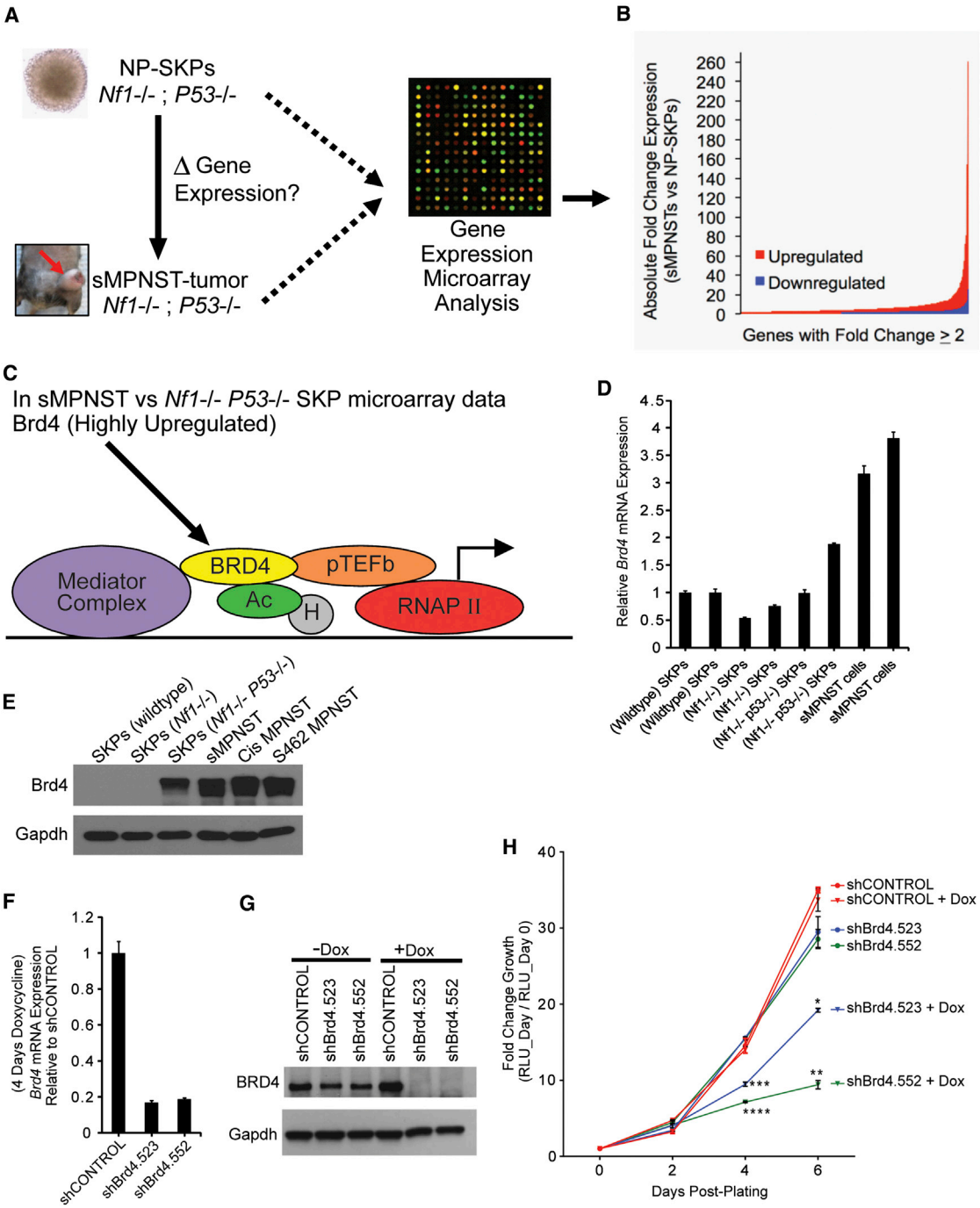

Figure 1. Identification of *Brd4* Upregulation and Roles in MPNSTs

(A) Diagram of microarray experiment for transcriptome analysis.

(B) Bar graph representation of the absolute fold change in expression of all genes from microarray experiment with fold change of ≥2.

(C) Pictorial representation of positive regulators of transcriptional elongation by RNA polymerase II and identification of Brd4 upregulation in MPNSTs (from microarray experiment).

(D and E) qRT-PCR and western blot analysis of MPNST cells and precursors for expression of *Brd4*.

(F and G) qRT-PCR and western blot analysis for *Brd4* knockdown in sMPNST-pTripz cells with or without doxycycline (Dox).

(H) Effect of *Brd4* shRNA induction on MPNST cell growth/viability using ATP CellTiter Glo assay.

All statistics are represented as the mean ± SEM (*p ≤ 0.05, **p ≤ 0.01, ***p ≤ 0.001, ***p ≤ 0.0001).

transcriptional elongation (Donner et al., 2010; Jang et al., 2005; Wu and Chiang, 2007) (Figure 1C). BRD4 has been previously implicated in cancer biology (Dawson et al., 2011; Delmore et al., 2011; Filippakopoulos et al., 2010; Firestein et al., 2008; Lovén et al., 2013; Zuber et al., 2011) and is currently amenable to pharmacological inhibition through small molecule bromodomain inhibitor JQ1 (Filippakopoulos et al., 2010), which may present a novel therapeutic modality for treating NF1-associated MPNSTs. Thus, we focused on elucidating the role of BRD4 in MPNSTs.

Brd4 Is Critical for Growth and Tumorigenic Capacity of MPNSTs

We sought to dissect the function of BRD4 in MPNSTs by employing a doxycycline (Dox)-inducible small hairpin RNA (shRNA) system to acutely knockdown *Brd4* mRNA levels. sMPNST cells were transduced with lentivirus harboring either scrambled shRNA (pTripz-shCONTROL) or *Brd4* shRNAs (pTripz-shBrd4.523 or pTripz-shBrd4.552), and then treated with puromycin to select for stably infected cells. Treatment of these cells with doxycycline to induce shRNA expression reveals >80% reduction of *Brd4* mRNA levels via *Brd4* shRNAs compared to scrambled shRNA (shCONTROL) induction, which is consistent with protein levels (Figures 1F and 1G). To evaluate the effect of acute depletion of *Brd4* on sMPNST cellular growth, we evaluated ATP levels as a surrogate for cell numbers before and after acute knockdown of *Brd4* and observed significantly reduced growth upon *Brd4* shRNA induction with doxycycline (Figure 1H).

To study the influence of BRD4 on the tumorigenic capacity of MPNST cells, we subcutaneously injected pTripz-shCONTROL and pTripz-shBrd4 sMPNST cells (Luciferase tagged) into nude mice. Two days later, both scrambled and *Brd4* shRNAs were turned on in sMPNST allografts by administration of doxycycline (1 mg/ml) through drinking water of the mice. By 30 days of shRNA induction in vivo, we found that *Brd4* shRNA-sMPNST cells had significantly delayed tumor burden/progression compared to control as indicated by periodic measurements of tumor bioluminescence and volume and final weight of excised tumors (Figures 2A–2E). Remarkably, induction of *Brd4* shRNA expression in established tumors (30 days after subcutaneous implantation) halted sMPNST tumor progression/growth when compared to shCONTROL sMPNST tumors (Figures 2F and 2G). Western blot analysis of these tumors indicates that these findings are consistent with reduced BRD4 protein levels in shBrd4+Dox tumors (Figure 2H). Through molecular analysis of tumor proliferation, we found that shBrd4 tumors had significantly fewer bromodeoxyuridine (BrdU)-positive cells than shCONTROL tumors (Figures 2I and 2J). All together, these data indicate an important role for BRD4 in maintaining tumorigenic capacity of MPNSTs in vivo.

Pharmacological Inhibition of Brd4 Suppresses MPNST Growth and Tumorigenesis

The remarkable inhibition of MPNST tumorigenesis through *Brd4* knockdown prompted us to evaluate the effect of inhibiting BRD4 with small molecule BET bromodomain inhibitor JQ1 (Filippakopoulos et al., 2010). We tested the effect of JQ1 on pretumorigenic NP-SKPs, sMPNST cells, and *cis* MPNST cells (derived from spontaneous MPNST arising in *cis* $Nf1^{+/-}$ $P53^{+/-}$ mice) (Mo et al., 2013; Vogel et al., 1999). All MPNST cells and NP-SKPs had decreased cellular viability/growth in a JQ1 dose-dependent manner with IC_{50} values less than 400 nM, whereas SKPs (both wild-type and *Nf1* null) were relatively unaffected (Figure 3A). These data may suggest a role for BRD4 in maintaining in vitro growth and survival signaling propagated by loss of both *Nf1* and *P53* in MPNSTs and their pretumorigenic precursors (NP-SKPs). Collectively, these promising findings suggest that JQ1 may have important therapeutic value in the treatment of MPNSTs.

In that regard, to investigate the therapeutic efficacy of JQ1 on MPNST tumor progression, we generated palpable (50 mm^3 average) sMPNST allografts (luciferase expressing) in 14 nude mice (two tumors per mouse). Prior to drug administration, we measured tumor volume and bioluminescence to separate tumor-bearing mice into two groups (14 tumors per group), in which tumor size and mouse gender/weight are equally represented (Figure 3B). Mice were treated with either vehicle or JQ1 for 15 days and then sacrificed. During this treatment period, we found that growth of all JQ1-treated tumors (n = 14) had been severely blunted compared to vehicle-treated tumors (n = 14) as indicated by delayed progression of tumor bioluminescence and volume (Figures 3C and 3D). Interestingly, during the course of the experiment, we observed sMPNST tumor regression in JQ1-treated mice both visually and through bioluminescence imaging (Figure 3E). Remarkably, we observed 50% to near complete regression of tumor volume in as little as 10 days of JQ1 treatment, which resulted in much smaller tumors compared to vehicle tumors (Figures 3F and 3G). Moreover, analysis of tumor proliferation revealed significantly fewer BrdU-positive cells in JQ1-treated sMPNST allografts compared to vehicle (Figures 3H and 3I). Importantly, we observed no significant changes in body weight nor behavior of mice during JQ1 treatment (data not shown), which is consistent with JQ1 tolerance observed in published mouse studies (Cheng et al., 2013; Delmore et al., 2011; Filippakopoulos et al., 2010; Zuber et al., 2011). These data strongly suggest great therapeutic potential for JQ1 in the treatment of NF1-associated MPNSTs.

Brd4 Regulates MPNST Cell-Cycle Progression and Cyclin D1 Expression

To gain insight into the mechanism of action for BRD4 in MPNST tumorigenesis, we first evaluated the effect of genetic and pharmacological inhibition of BRD4 on sMPNST cell number. On average, we found that induction of *Brd4* shRNAs led to 60%–65% reduction in cell number after 5 days in culture compared to cells without induction or shCONTROL cells (Figure 4A). We observed a similar effect on sMPNST cells treated 4 days with JQ1 (Figure 4B). These data suggested inhibition of MPNST proliferation through BRD4 inhibition. Indeed, we found that BRD4 inhibition restrains MPNST cell-cycle progression. Analysis of proliferation via BrdU incorporation and DNA content by flow cytometry led us to find that BRD4 depletion leads to significant reduction of BrdU incorporation, a predominant increase in percentage of cells in G1

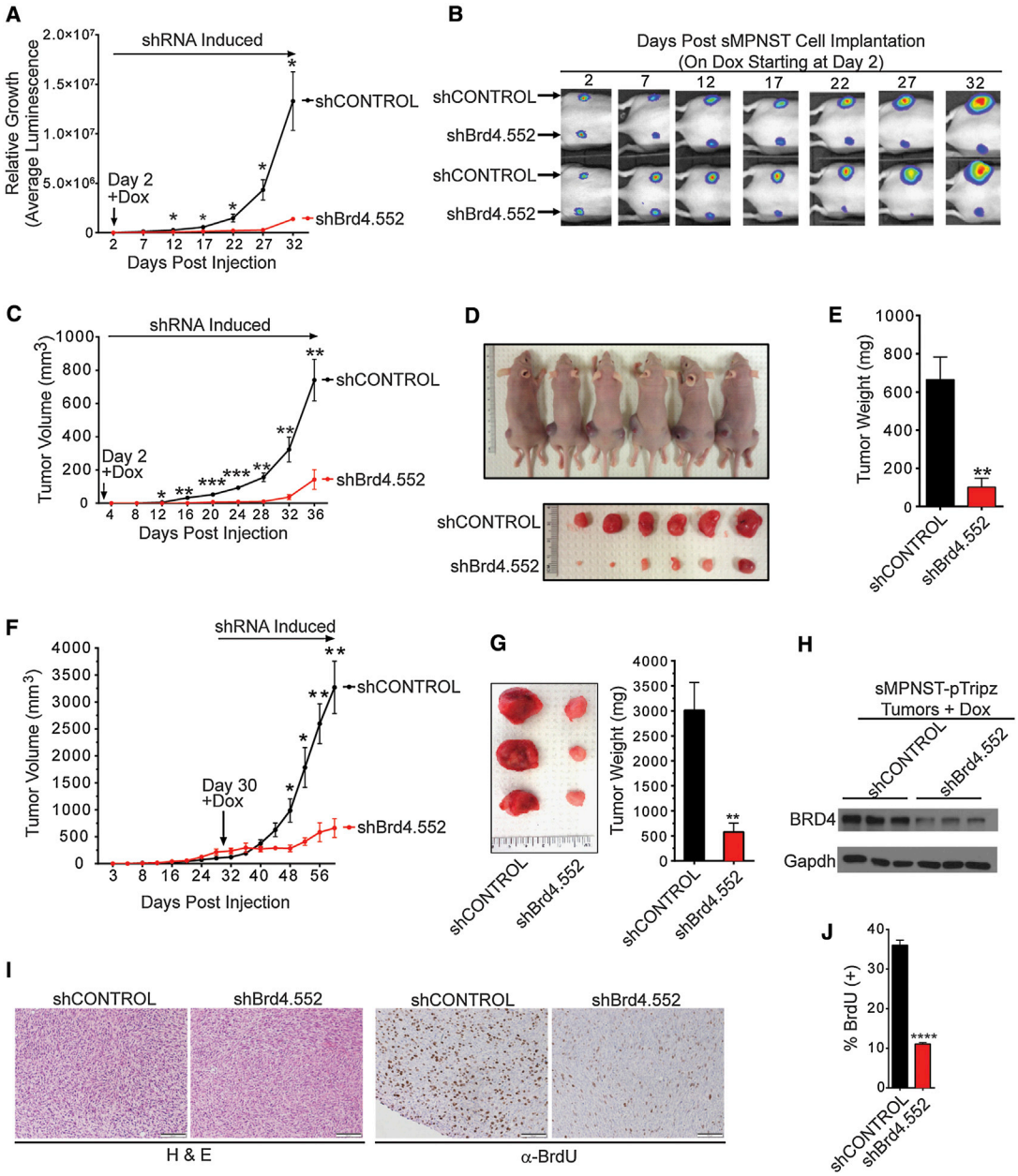

Figure 2. BRD4 Maintains Tumorigenic Capacity of MPNSTs In Vivo

(A) Growth of shCONTROL and shBrd4.552 sMPNST tumors relative to "day 2" value. Values represent luminescence counts (tumor bioluminescence imaging, n = 6 tumors per group).

(B) Representative pictures of sMPNST tumor bioluminescence in mice over time, which indicate that acute *Brd4* knockdown suppresses MPNST tumorigenesis in vivo. Mice were started on doxycycline water on day 2 and kept on this treatment until the end of the experiment.

(C) sMPNST tumor volume measurements (each data point represents the average measurement from six different tumors per group).

(D) Top panel: mice at 36 days postsubcutaneous implantation of sMPNST tumor cells (shCONTROL on left flank and shBrd4.552 on right flank). Bottom panel: tumors excised from mice in the top panel.

(E) Average weight of excised tumors from bottom panel of Figure 3D.

(F) Tumor volume of shCONTROL and shBrd4.552 sMPNST-pTripz tumors in mice. At day 30, when tumors were established (200–400 mm^3), mice were started on doxycycline water.

(G) Representative picture and average weight of excised sMPNST tumors from end of experiment in Figure 3F.

(H) Western blot analysis of BRD4 protein levels in shCONTROL and shBrd4.552 sMPNST tumors in mice given doxycycline water.

(I) Representative images of sMPNST tumor sections stained with either hematoxylin and eosin (H&E) or BrdU antibody.

(J) Quantification of the percentage of BrdU(+) cells from sMPNST tumor sections (scale bars represent 100 μm). All statistics are represented as the mean ± SEM (*$p \leq 0.05$, **$p \leq 0.01$, ***$p \leq 0.001$, ***$p \leq 0.0001$).

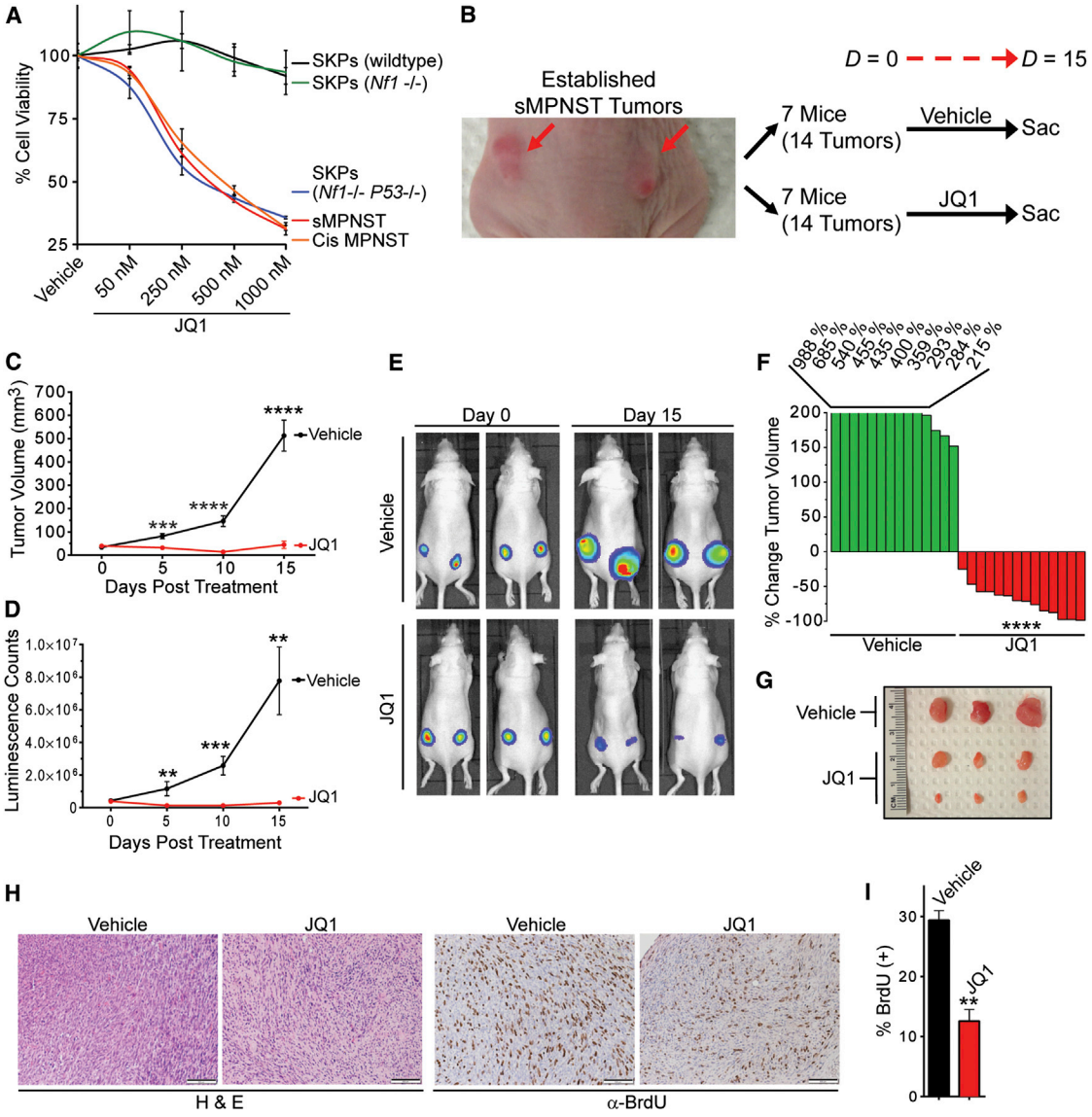

Figure 3. JQ1 Induces MPNST Regression In Vivo

(A) Dose-response curves for 2 day JQ1 treatment on primary murine SKPs (wild-type, *Nf1*$^{-/-}$, *Nf1*$^{-/-}$ *P53*$^{-/-}$) and MPNST cells (SKP model and *cisNP* model). ATP CellTiter-glo assay was used to measure cell viability and normalized to DMSO (vehicle) for each cell type.

(B) Overview of JQ1 drug trial with nude mice bearing sMPNST allografts.

(C) Average sMPNST tumor volume measured during JQ1 drug trial (n = 14 tumors per treatment group).

(D) Average sMPNST tumor bioluminescence counts measured during JQ1 drug trial (n = 14 tumors per treatment group).

(E) Bioluminescence imaging of sMPNST allografts in mice before and after the JQ1 drug trial.

(F) Waterfall plot showing the percentage change in sMPNST tumor volume from before starting (day 0) and after 10 days of JQ1 treatment.

(G) Representative pictures of sMPNST allografts excised from mice treated with vehicle or JQ1 for 15 days.

(H) Staining of sections from sMPNST allografts (vehicle or JQ1 treated) with hematoxylin and eosin (H&E) or immunostaining with BrdU antibody.

(I) Quantification of BrdU(+) cells from vehicle- and JQ1-treated sMPNST tumor sections (scale bars represent 100 μm). All statistics are represented as the mean ± SEM (*p ≤ 0.05, **p ≤ 0.01, ***p ≤ 0.001, ***p ≤ 0.0001).

phase, and modest affect on the percentage of cells in G2/M phase (Figure 4C). We observed similar results in both sMPNST cells and S462 human MPNST cells treated with JQ1 (Figures 4C and 4D). Collectively, these data suggest that genetic and pharmacological inhibition of BRD4 impedes MPNST cell-cycle progression.

Previously, we and others described a role for the CXCR4/β-catenin signaling pathway in stimulating MPNST cell-cycle progression via control of *Cyclin D1* mRNA expression, which highlights the importance of *Cyclin D1* maintenance in MPNST cell-cycle control (Mo et al., 2013). How *Cyclin D1* transcription is regulated in MPNSTs remains unknown, but previous reports

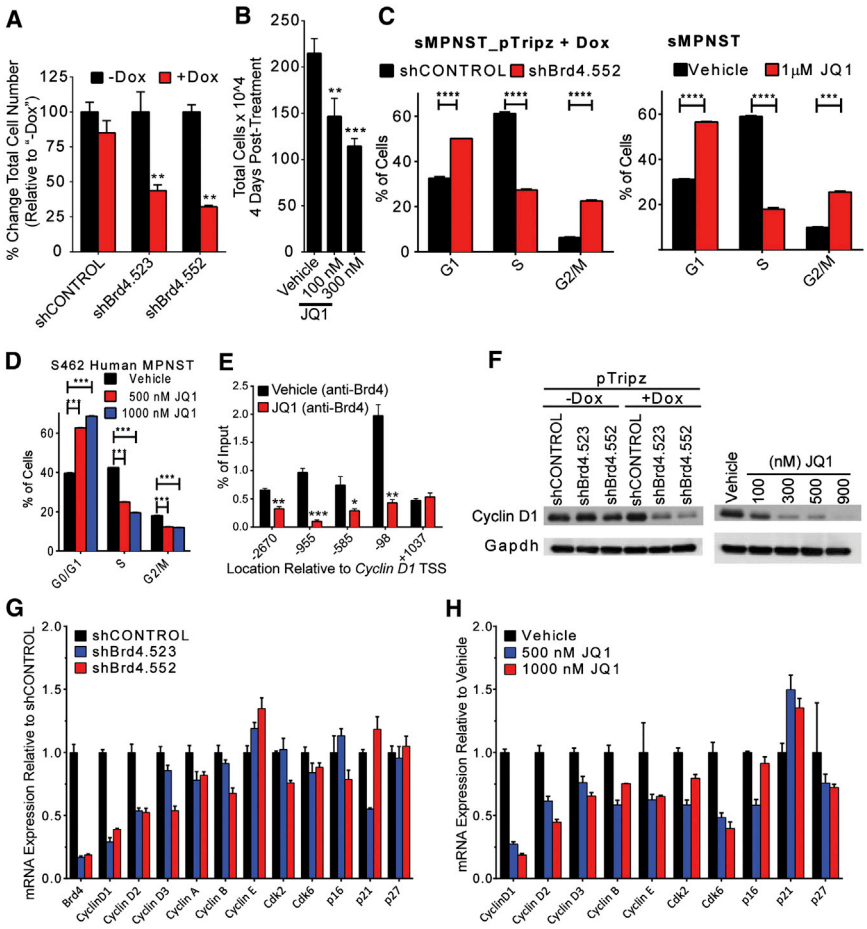

Figure 4. BRD4 Maintains Cyclin D1 Expression and Cell-Cycle Progression in MPNSTs

(A) sMPNST cells harboring doxycycline (Dox)-inducible shRNAs were counted after 5 days culture (+ or – Dox) and normalized to cell count of "-Dox" cells.

(B) sMPNST cells were counted 4 days after culturing in the presence of vehicle (DMSO) or JQ1.

(C) sMPNST cells were harvested 4 days after *Brd4* shRNA induction or 3 days after JQ1 treatment for processing, and subsequent analysis of BrdU uptake and DNA content by flow cytometry was conducted to determine the percentage of cells in the indicated cell-cycle phases.

(D) Cell-cycle analysis of 48 hr treated S462 cells through flow cytometry for BrdU(+) cells and DNA content (PI).

(E) sMPNST cells treated 24 hr with vehicle or 1,000 nM JQ1 were harvested for chromatin immunoprecipitation (ChIP)-PCR analysis at different regions relative to *Cyclin D1* transcription start site (TSS).

(F) Western blot analysis of Cyclin D1 protein levels in sMPNST cells with *Brd4* knockdown or JQ1 treatment.

(G and H) qPCR analysis of cell-cycle regulatory genes in sMPNST cells with Brd4 knockdown or JQ1 treatment, respectively.

All statistics are represented as the mean ± SEM (*$p \leq 0.05$, **$p \leq 0.01$, ***$p \leq 0.001$, ***$p \leq 0.0001$).

indicate *Cyclin D1* as a potential target of BRD4 (Mochizuki et al., 2008; Yang et al., 2008). Therefore, we sought to determine if BRD4 directly regulates *Cyclin D1* transcription in MPNSTs. Through chromatin immunoprecipitation quantitative PCR (ChIP-qPCR) analysis, we found that BRD4 occupies the promoter of *Cyclin D1*, and that displacement of BRD4 from chromatin by JQ1 treatment led to reduced promoter occupancy in sMPNST cells (Figure 4E). Consequently, we found that shRNA-mediated knockdown or pharmacological inhibition of BRD4 leads to substantial decrease in *Cyclin D1* mRNA and protein abundance in MPNST cells, whereas other cell-cycle regulators are less affected by *Brd4* shRNA or JQ1 in sMPNST cells (Figures 4F–4H). Together, these data point to a mechanism of BRD4-mediated epigenetic control of *Cyclin D1* transcription and suggest BRD4 as a therapeutic target for inhibiting oncogenic Cyclin D1 in MPNSTs.

Brd4 Regulates Expression of Proapoptotic Bim

Cell-cycle arrest can lead to subsequent cellular apoptosis (Pietenpol and Stewart, 2002). Further analysis of acute knockdown of *Brd4* in MPNST led us to observe increased floating cells in culture (Figure 5A), which was suggestive of apoptosis induction. Indeed, we found an increase in apoptotic cells and activation of apoptotic markers in both mouse and human MPNST cells with BRD4 inhibition (Figures 5B–5D). On the other hand, we observed that both wild-type SKPs and *Nf1*$^{-/-}$ SKPs do not undergo robust apoptosis when treated with JQ1 (Figure S2). To elucidate how BRD4 inhibition triggers apoptosis of MPNSTs, we performed gene expression microarray analysis to first identify differentially expressed genes in MPNST cells with or without BRD4 inhibition (both shRNA and JQ1), which led us to identify upregulation of proapoptotic BIM (*Bcl2l11*) (Figure 5E). We also found that BRD4 inhibition decreased expression of antiapoptotic *Bcl2* in our microarray data (data not shown). Quantitative RT-PCR and western blot analyses confirm that BRD4 inhibition (shRNA or JQ1) leads to induction of BIM and downregulation of BCL-2, and relatively minor effect on the expression of additional apoptosis regulators evaluated (Figures 5F and 5G). BIM is a proapoptotic, BH3-domain-containing protein that is thought to play a central role in apoptosis through activation of proapoptotic BAX and BAK, which leads to mitochondrial permeabilization that is followed by activation of caspases and apoptosis (Bean et al., 2013; Tait and Green, 2010; Wei et al., 2001). BCL-2 is an antiapoptotic protein that is thought to prevent BAX/BAK activation (Cheng et al., 2001). One of the mechanisms is through inhibition/sequestration of proapoptotic BH3-only proteins, such as BIM and PUMA (Cheng et al., 2001; Letai et al., 2002; Youle and Strasser, 2008).

To determine if BRD4-inhibition-mediated downregulation of *Bcl2* expression promotes MPNST apoptosis, we treated

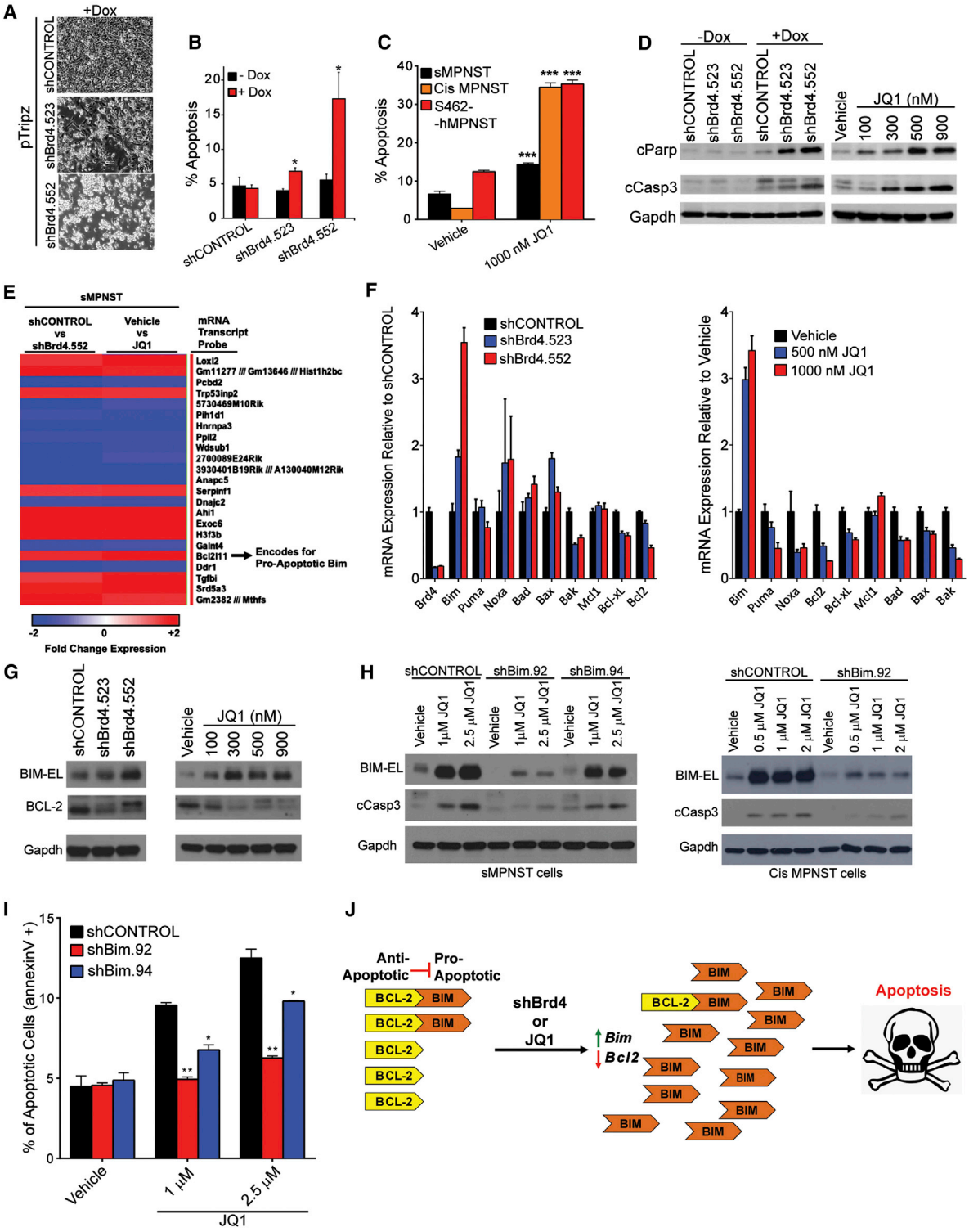

Figure 5. BET Bromodomain Inhibition Triggers MPNST Apoptosis through *Bim* Induction

(A) Microscopy images of sMPNST cells after 5 days of shRNA induction in vitro.

(B) Percentage apoptosis in sMPNST cells with and without *Brd4* shRNA induction (5 days) by flow cytometry analysis of Annexin V (+) cells.

(C) Apoptosis induction by 3 days of JQ1 treatment in mouse and human MPNSTs cells through flow cytometry analysis for Annexin V (+) cells.

(D) Western blot analyses of lysates from sMPNST cells with (3 days) *Brd4* knockdown or (2 days) JQ1 treatment for activation of apoptosis (cCasp3 = cleaved caspase 3, cParp = cleaved Parp).

(legend continued on next page)

MPNST cells with ABT-263, a selective small molecule that inhibits BCL-2/BCL-X_L, which prevents sequestration of proapoptotic BIM or PUMA. We found that BCL-2/BCL-X_L inhibition with ABT-263 is not sufficient to trigger robust apoptosis of MPNST cells (Figure S4), which suggests that perhaps inhibition of BRD4 leading to induction of *Bim* initiates MPNST apoptosis. Indeed, we found that constitutive knockdown of *Bim* attenuates/rescues JQ1-induced apoptosis in multiple MPNST cell types as indicated by reduced caspase-3 cleavage and fewer apoptotic cells (Figures 5H and 5I). Collectively, these findings lead us to propose a model in which BRD4 inhibition or JQ1 treatment initiates apoptosis through induction of proapoptotic *Bim*, and suppression of antiapoptotic *Bcl2* to trigger apoptosis of NF1-associated MPNSTs (Figure 5J). Furthermore, the dual restraint on proliferation and survival may indicate how BRD4 inhibition is exquisitely effective against MPNSTs.

DISCUSSION

Here, we employed a mouse model of MPNST that allowed us to study the evolution of these tumors at the transcriptome level, which permitted us to identify and elucidate a mechanistic basis for Brd4 in maintaining the tumorigenic capacity and survival of MPNSTs. Importantly, this study translates basic insights into a therapeutically tractable target for impeding the progression and survival of incurable NF1-associated MPNSTs, which may represent a significant paradigm shift for MPNST patient therapy. We also provide a mechanism of action as a framework for developing new therapeutic strategies to disarm remaining cell-survival networks that MPNSTs may rely upon.

Although traditional Genetic Engineered Mouse Models (GEMMs) with loss of tumor suppressors *Nf1* and *P53* have provided a genetic basis for MPNST pathogenesis, their utility for discovering therapeutic targets to impede both progression and survival of these tumors has remained limited. In addition, the traditional route to study the function of additional genes in a GEMM would require generating new mouse strains (knockout, knockin, or conditional alleles), which incurs a longer time horizon and costs toward studying gene function (Heyer et al., 2010). Moreover, if one wishes to study gene expression at different stages of tumor evolution, isolation of relatively homogenous cells from spontaneously arising tumors in traditional GEMMs would prove difficult (Heyer et al., 2010). Although SKPs are a cell of origin for dermal neurofibromas, at present it is not clear that SKPs are a cell of origin for MPNSTs in humans. Nevertheless, observing that $Nf1^{-/-}$ $P53^{-/-}$ SKPs can undergo malignant transformation to MPNSTs suggested a novel opportunity to delineate what molecular changes underlie MPNST development. Thus, in this study, we took advantage of our nongermline GEMM of NF1-associated MPNST to study the transcriptome of relatively homogenous sMPNSTs and their pretumorigenic precursors (NP-SKPs). The elevated expression of *Brd4* in our sMPNST transcriptome data captured our attention. Our ability to genetically and pharmacologically inhibit BRD4 in a temporal manner with great haste and ease in our stem/progenitor transplantation model allowed us to elucidate the role of BRD4 in MPNST tumorigenesis. These results highlight the strength and speed in which our nongermline GEMM can accelerate discovery of tractable therapeutic targets for rare malignancies that represent an unmet medical need.

As a proof of principle, using this sMPNST model, we and our colleagues previously delineated a signaling pathway in which cell-surface receptor CXCR4 mediates intracellular activation of β-catenin, which leads to expression of Cyclin D1 and established a critical role for Cyclin D1 in promoting cell-cycle progression and tumorigenesis of MPNSTs (Mo et al., 2013). In agreement, another group identified Wnt/β-catenin signaling as a potential driver of MPNSTs through a *Sleeping Beauty* genetic screen and found that this pathway regulates Cyclin D1 expression in MPNSTs as well (Rahrmann et al., 2013; Watson et al., 2013). In the current study presented here, we demonstrate that BRD4 occupies the promoter of *Cyclin D1* in MPNSTs, and that pharmacological inhibition with JQ1 inhibits BRD4 occupancy at that promoter leading to decreased expression of *Cyclin D1*, which correlates with decreased proliferation observed. In contrast, BRD4 has been shown to be required for maintaining transcription of oncogenic *c-Myc* in hematopoietic malignancies, but we did not observe loss of *c-Myc* expression in MPNSTs with BRD4 inhibition (data not shown). This cancer cell type specificity for regulating tumor oncogenes through BRD4 can now be attributed to the recent discovery of BRD4-regulated superenhancers in multiple myeloma and other cancers (Lovén et al., 2013). Those findings suggest that BRD4 may maintain the cancer cell state through transcriptional regulation of specific oncogenes depending on the cell type of origin (*c-Myc* in the case of leukemia and multiple myeloma, and *Cyclin D1* in NF1-associated MPNSTs) (Delmore et al., 2011; Zuber et al., 2011).

Most importantly, our findings point to a mechanism of action by which bromodomain inhibition induces apoptosis through induction proapoptotic effector molecule BIM. We demonstrate that knockdown of *Bim* can rescue MPNST cells from JQ1-induced apoptosis, which further highlights the importance of this finding. Interestingly, in support for the role of Bim in MPNST tumor development, we observed that sMPNST cells with Bim knockdown had elevated tumor bioluminescence when compared control sMPNST cells. Thus, further highlighting the importance of Bim regulation through BRD4 (Figure S3).

Albeit, additional mechanisms underlying JQ1-induced death in MPNSTs may exist. For example, we observed downregulation of *Bcl2* expression in BRD4-inhibited MPNSTs, which is

(E) Expression microarray analysis comparing the effect of *Brd4* shRNA or JQ1 on sMPNST cells reveals induction of proapoptotic effector *Bim*.
(F) qPCR analysis of the effect of (3 days) *Brd4* shRNA or (2 days) JQ1 treatment on the expression of apoptosis regulators in sMPNST cells.
(G) Western blot validation of BIM induction and BCL-2 downregulation through *Brd4* shRNA (3 days) or JQ1 (2 days) treatment in sMPNST cells.
(H) Western blot analysis of BIM knockdown leading to attenuation of cleaved caspase 3 in sMPNST and *Cis* MPNST cells treated with JQ1 (2 days).
(I) Flow cytometry analysis of Annexin V (+) cells reveals attenuated apoptosis through *Bim* shRNAs in sMPNST cells treated with JQ1 for 4 days.
(J) Model for how BET bromodomain inhibition modulates the ratio of proapoptotic and antiapoptotic molecules in favor of apoptosis.
All statistics are represented as the mean ± SEM (*$p \leq 0.05$, **$p \leq 0.01$, ***$p \leq 0.001$, ***$p \leq 0.0001$).

consistent with a study involving bromodomain inhibition in MLL-fusion leukemia (Dawson et al., 2011). However, through direct inhibition of BCL-2 using ABT-263 we did not observe significant apoptosis compared to JQ1, which suggests that BCL-2 inhibition alone does not induce MPNST apoptosis robustly, but, in combination with BIM induction, can efficiently induce apoptosis. Our observations suggest that bromodomain inhibition with JQ1 induces *Bim* and downregulates *Bcl2* expression, leading to an imbalance of pro- and antiapoptotic effectors that favors induction of apoptosis (Figure 5J), and supports the model for an antiapoptotic/proapoptotic BCL-2 rheostat (Bean et al., 2013; Corcoran et al., 2013). Consistent with this idea, we found that further inhibition of BCL-2 with ABT-263 synergizes with JQ1 or shBrd4 to more potently induce MPNST apoptosis (Figure S4).

On the other hand, we observed that a majority of JQ1-regulated genes do not overlapping with shBrd4-regulated genes (Figure S5), which is expected given that JQ1 also inhibits Brd2 and Brd3. It remains unknown whether additional BET bromodomain proteins (BRD2, BRD3) (also targeted by JQ1) play a role in MPNST pathogenesis. However, in our *Nf1*$^{-/-}$ *P53*$^{-/-}$ SKP and MPNST microarray data, differential expression of neither Brd2 nor Brd3 was observed, which is contrary to what we observed for Brd4 (data not shown). Nonetheless, the role of additional BET bromodomain family members (including Brd2 and Brd3) will be of interest in future studies, but at present, it remains clear from our findings that BIM induction plays a central role in shBrd4/JQ1-induced apoptosis in MPNSTs. More broadly, these findings suggest an epigenetic mechanism underlying the balance of pro-apoptotic/antiapoptotic proteins that can be exploited by BET bromodomain inhibitors for inducing cancer cell apoptosis.

All together, the dual effect of growth inhibition and apoptosis leading to tumor regression via JQ1 may allow physicians to utilize JQ1 along with surgery to better manage these tumors in NF1 patients. Although JQ1 remains to be optimized for clinical development, its equivalent bromodomain inhibitor I-BET 151 is currently being evaluated in phase I clinical trials and we hope will reach patients in the clinic (http://www.clinicaltrials.gov). Future studies to molecularly understand how JQ1 induces proapoptotic *Bim* should lead to new targets or additional approved drugs for therapeutically inducing this apoptotic pathway, and we speculate those studies would allow more rapid or synergistic induction of tumor regression. Therefore, this may allow physicians to limit drug exposure to patients while maintaining or boosting therapeutic efficacy.

In conclusion, we took advantage of an MPNST mouse model that permits the study of tumor evolution for transcriptome analysis, which allowed us to identify and elucidate mechanisms for BRD4 in MPNST growth and survival. Our findings collectively provide a strong preclinical basis for evaluating BET bromodomain inhibitors as novel therapies for these life-threatening MPNSTs in NF1 patients.

EXPERIMENTAL PROCEDURES

Cells and Reagents

Primary sMPNST and *Cis* MPNST cells were established from SKP-MPNST and *cis*NP model mice as described (Mo et al., 2013; Vogel et al., 1999). S462 human MPNST cell line is a gift from Dr. Karen Cichowski (Brigham and Women's Hospital, MA). All MPNST cells (mouse and human) are cultured in DMEM (10% fetal bovine serum, 1% penicillin-streptomycin, 1% L-glutamine, 1% sodium pyruvate). SKPs were prepared and cultured as described (Biernaskie et al., 2006).

Animal Studies

All mice were housed in the animal facility at the University of Texas Southwestern Medical Center at Dallas (UTSW). Animal care and use were in compliance with regulations of the Institutional Animal Care and Research Advisory Committee at UTSW. Athymic nude mice were used for tumor studies. For shRNA induction in sMPNST-pTripz tumors in vivo, mice were given water containing 1 mg/ml doxycycline (Sigma-Aldrich) in 5% sucrose. For daily drug administration, a single dose of vehicle or 50 mg/kg JQ1 (Cayman Chemical) were prepared as described (Filippakopoulos et al., 2010; Zuber et al., 2011). Tumor volume was calculated as described (Mo et al., 2013). D-Luciferin (50 mg/kg) was administered by intraperitoneal injection followed by bioluminescent imaging of mice 10 min later with IVIS Spectrum system (Caliper Life Sciences).

Lentiviral Constructs

Mouse *Brd4* shRNAs were generated by synthesizing 22-mer sequences corresponding to *Brd4* shRNAs described previously (Zuber et al., 2011) for PCR cloning into pTripz lentiviral vector. For lentivirus production, psPAX2 and pMD2.g (Addgene plasmids 12260 and 12259) packaging vectors were used.

In Vitro Growth Assays

ATP CellTiter Glo assay (Promega) was performed as per manufacturer's instructions. The FLUOstar OPTIMA 96-well plate reader (BMG Labtech) was used for luminescence measurements.

BrdU Cell-Cycle Analysis and Annexin V Flow Cytometry

Cell-cycle studies were conducted using BrdU Flow kit (BD Biosciences) as per manufacturer's instructions. For analysis of cellular apoptosis/death, Annexin V-FITC Kit (Miltenyi Biotec) was used as per manufacturer's instructions. All flow cytometry was performed using FACSCalibur Flow Cytometer (BD Biosciences) at the UTSW Flow Cytometry core facility. Data were analyzed using FlowJo software (Tree Star).

RNA Isolation, cDNA Synthesis, qRT-PCR

RNEasy mini kit (QIAGEN) was used to isolate total RNA from cells, followed by cDNA synthesis with iScript Select cDNA synthesis kit (Bio-Rad), and then qRT-PCR using iTaq Universal SYBR Green Supermix (Bio-Rad) on the CFX Connect Real-Time PCR platform (Bio-Rad). Data were quantified by ΔCt method and normalized relative to Gapdh. See Figure S6 for primers used.

Expression Microarray Analysis

For Figure 1, total RNA was isolated from sMPNST tumors and NP-SKPs from which those tumors were derived from (three biological replicates were prepared for both groups). For microarray analysis of shBrd4 and JQ1 effect on sMPNST cells, technical replicates (n = 3) were used for the experiment. RNA quality and microarray experiments using Mouse Genome 430 2.0 microarrays (Affymetrix) were conducted by the UT Southwestern Microarray core facility. Data were analyzed with GeneSpring GX software (Agilent Technologies).

Western Blot

Protein isolation and subsequent western blot analysis were performed as described previously (Mo et al., 2013). Antibodies used were as follows: BRD4 (Epitomics, Bethyl Labs); BIM, Cleaved Caspase-3 (Cell Signaling Technology); Cleaved Parp, Cyclin D1 (Millipore); and Bcl2, Gapdh (Santa Cruz Biotechnology).

Immunohistochemistry

Tumor tissue sample preparation, immunohistochemistry, and data quantification was performed as described previously (Mo et al., 2013). Antibodies used were BRD4 (Bethyl Laboratories) and BrdU (Dako).

Chromatin-Immunoprecipitation qPCR

ChIP experiments were conducted as described in detailed protocol from Abcam. Briefly, chromatin equivalent to 25 μg DNA was 10-fold diluted in IP dilution buffer, precleared by 1 hr incubation with ChIP-Grade Protein A/G Plus Agarose beads (Thermo Scientific), and then incubated overnight with Brd4 or control immunoglobulin G (IgG) antibody, 2 hr with protein A/G agarose beads, followed by wash, elution, and DNA purification (phenol/chloroform extraction followed by ethanol precipitation). For qPCR analysis, each IP signal was normalized to input signal to plot data as percentage of input. Antibodies used were as follows: BRD4 (Bethyl Labs) and control IgG (Cell Signaling Technology).

Statistical Analyses

All data are displayed as the mean ± SEM unless specified otherwise. A two-tailed t test was used to evaluate statistical significance ($p < 0.05$ was deemed statistically significant).

ACCESSION NUMBERS

GEO accession number for data in this paper is GSE50865.

SUPPLEMENTAL INFORMATION

Supplemental Information includes six figures and can be found with this article online at http://dx.doi.org/10.1016/j.celrep.2013.12.001.

ACKNOWLEDGMENTS

We thank all members of the Le lab and Wei Mo for helpful suggestions and discussions. A.J.P. is a recipient of the Young Investigator Award from Children Tumor Foundation. L.Q.L. holds a Career Award for Medical Scientists from the Burroughs Wellcome Fund. This work was partially supported by funding from the Dermatology Foundation, Disease-Oriented Clinical Scholar Program, National Cancer Institute of the National Institutes of Health grant no. R01 CA166593, and U.S. Department of Defense grant no. W81XWH-12-1-0161 to L.Q.L.

Received: July 19, 2013
Revised: September 25, 2013
Accepted: December 3, 2013
Published: December 26, 2013

REFERENCES

Albers, A.C., and Gutmann, D.H. (2009). Gliomas in patients with neurofibromatosis type 1. Expert Rev. Neurother. *9*, 535–539.

Albritton, K., Rankin, C., Coffin, C., Ratner, N., Budd, G., Schuetze, S., Randall, R., Declue, J., and Borden, E. (2006). Phase II study of erlotinib in metastatic or unresectable malignant peripheral nerve sheath tumors (MPNST). J. Clin. Oncol. *24*, 9518.

Bajenaru, M.L., Hernandez, M.R., Perry, A., Zhu, Y., Parada, L.F., Garbow, J.R., and Gutmann, D.H. (2003). Optic nerve glioma in mice requires astrocyte Nf1 gene inactivation and Nf1 brain heterozygosity. Cancer Res. *63*, 8573–8577.

Bean, G.R., Ganesan, Y.T., Dong, Y., Takeda, S., Liu, H., Chan, P.M., Huang, Y., Chodosh, L.A., Zambetti, G.P., Hsieh, J.J.-D., and Cheng, E.H. (2013). PUMA and BIM are required for oncogene inactivation-induced apoptosis. Sci. Signal. *6*, ra20.

Biernaskie, J.A., McKenzie, I.A., Toma, J.G., and Miller, F.D. (2006). Isolation of skin-derived precursors (SKPs) and differentiation and enrichment of their Schwann cell progeny. Nat. Protoc. *1*, 2803–2812.

Chau, V., Lim, S.K., Mo, W., Liu, C., Patel, A.J., McKay, R.M., Wei, S., Posner, B.A., De Brabander, J.K., Williams, N.S., et al. (2013). Preclinical therapeutic efficacy of a novel pharmacological inducer of apoptosis in malignant peripheral nerve sheath tumors. Cancer Res. Published online November 27, 2013.

Cheng, E.H.Y.A., Wei, M.C., Weiler, S., Flavell, R.A., Mak, T.W., Lindsten, T., and Korsmeyer, S.J. (2001). BCL-2, BCL-X(L) sequester BH3 domain-only molecules preventing BAX- and BAK-mediated mitochondrial apoptosis. Mol. Cell *8*, 705–711.

Cheng, Z., Gong, Y., Ma, Y., Lu, K., Lu, X., Pierce, L.A., Thompson, R.C., Muller, S., Knapp, S., and Wang, J. (2013). Inhibition of BET bromodomain targets genetically diverse glioblastoma. Clin. Cancer Res. *19*, 1748–1759.

Cichowski, K., Shih, T.S., Schmitt, E., Santiago, S., Reilly, K., McLaughlin, M.E., Bronson, R.T., and Jacks, T. (1999). Mouse models of tumor development in neurofibromatosis type 1. Science *286*, 2172–2176.

Corcoran, R.B., Cheng, K.A., Hata, A.N., Faber, A.C., Ebi, H., Coffee, E.M., Greninger, P., Brown, R.D., Godfrey, J.T., Cohoon, T.J., et al. (2013). Synthetic lethal interaction of combined BCL-XL and MEK inhibition promotes tumor regressions in KRAS mutant cancer models. Cancer Cell *23*, 121–128.

Dawson, M.A., Prinjha, R.K., Dittmann, A., Giotopoulos, G., Bantscheff, M., Chan, W.-I., Robson, S.C., Chung, C.W., Hopf, C., Savitski, M.M., et al. (2011). Inhibition of BET recruitment to chromatin as an effective treatment for MLL-fusion leukaemia. Nature *478*, 529–533.

Delmore, J.E., Issa, G.C., Lemieux, M.E., Rahl, P.B., Shi, J., Jacobs, H.M., Kastritis, E., Gilpatrick, T., Paranal, R.M., Qi, J., et al. (2011). BET bromodomain inhibition as a therapeutic strategy to target c-Myc. Cell *146*, 904–917.

Dey, A., Chitsaz, F., Abbasi, A., Misteli, T., and Ozato, K. (2003). The double bromodomain protein Brd4 binds to acetylated chromatin during interphase and mitosis. Proc. Natl. Acad. Sci. USA *100*, 8758–8763.

Donner, A.J., Ebmeier, C.C., Taatjes, D.J., and Espinosa, J.M. (2010). CDK8 is a positive regulator of transcriptional elongation within the serum response network. Nat. Struct. Mol. Biol. *17*, 194–201.

Duong, T.A., Sbidian, E., Valeyrie-Allanore, L., Vialette, C., Ferkal, S., Hadj-Rabia, S., Glorion, C., Lyonnet, S., Zerah, M., Kemlin, I., et al. (2011). Mortality associated with neurofibromatosis 1: a cohort study of 1895 patients in 1980-2006 in France. Orphanet J. Rare Dis. *6*, 18.

Endo, M., Kobayashi, C., Setsu, N., Takahashi, Y., Kohashi, K., Yamamoto, H., Tamiya, S., Matsuda, S., Iwamoto, Y., Tsuneyoshi, M., and Oda, Y. (2011). Prognostic significance of p14ARF, p15INK4b, and p16INK4a inactivation in malignant peripheral nerve sheath tumors. Clin. Cancer Res. *17*, 3771–3782.

Filippakopoulos, P., Qi, J., Picaud, S., Shen, Y., Smith, W.B., Fedorov, O., Morse, E.M., Keates, T., Hickman, T.T., Felletar, I., et al. (2010). Selective inhibition of BET bromodomains. Nature *468*, 1067–1073.

Firestein, R., Bass, A.J., Kim, S.Y., Dunn, I.F., Silver, S.J., Guney, I., Freed, E., Ligon, A.H., Vena, N., Ogino, S., et al. (2008). CDK8 is a colorectal cancer oncogene that regulates beta-catenin activity. Nature *455*, 547–551.

Gregorian, C., Nakashima, J., Dry, S.M., Nghiemphu, P.L., Smith, K.B., Ao, Y., Dang, J., Lawson, G., Mellinghoff, I.K., Mischel, P.S., et al. (2009). PTEN dosage is essential for neurofibroma development and malignant transformation. Proc. Natl. Acad. Sci. USA *106*, 19479–19484.

Heyer, J., Kwong, L.N., Lowe, S.W., and Chin, L. (2010). Non-germline genetically engineered mouse models for translational cancer research. Nat. Rev. Cancer *10*, 470–480.

Huijbregts, R.P.H., Roth, K.A., Schmidt, R.E., and Carroll, S.L. (2003). Hypertrophic neuropathies and malignant peripheral nerve sheath tumors in transgenic mice overexpressing glial growth factor β3 in myelinating Schwann cells. J. Neurosci. *23*, 7269–7280.

Jang, M.K., Mochizuki, K., Zhou, M., Jeong, H.-S., Brady, J.N., and Ozato, K. (2005). The bromodomain protein Brd4 is a positive regulatory component of P-TEFb and stimulates RNA polymerase II-dependent transcription. Mol. Cell *19*, 523–534.

Jessen, W.J., Miller, S.J., Jousma, E., Wu, J., Rizvi, T.A., Brundage, M.E., Eaves, D., Widemann, B., Kim, M.-O., Dombi, E., et al. (2013). MEK inhibition exhibits efficacy in human and mouse neurofibromatosis tumors. J. Clin. Invest. *123*, 340–347.

Johannessen, C.M., Johnson, B.W., Williams, S.M.G., Chan, A.W., Reczek, E.E., Lynch, R.C., Rioth, M.J., McClatchey, A., Ryeom, S., and Cichowski,

K. (2008). TORC1 Is Essential for NF1-Associated Malignancies. Curr. Biol. *18*, 56–62.

Joseph, N.M., Mosher, J.T., Buchstaller, J., Snider, P., McKeever, P.E., Lim, M., Conway, S.J., Parada, L.F., Zhu, Y., and Morrison, S.J. (2008). The loss of Nf1 transiently promotes self-renewal but not tumorigenesis by neural crest stem cells. Cancer Cell *13*, 129–140.

Keng, V.W., Rahrmann, E.P., Watson, A.L., Tschida, B.R., Moertel, C.L., Jessen, W.J., Rizvi, T.A., Collins, M.H., Ratner, N., and Largaespada, D.A. (2012). PTEN and NF1 inactivation in Schwann cells produces a severe phenotype in the peripheral nervous system that promotes the development and malignant progression of peripheral nerve sheath tumors. Cancer Res. *72*, 3405–3413.

King, A.A., Debaun, M.R., Riccardi, V.M., and Gutmann, D.H. (2000). Malignant peripheral nerve sheath tumors in neurofibromatosis 1. Am. J. Med. Genet. *93*, 388–392.

King, B., Trimarchi, T., Reavie, L., Xu, L., Mullenders, J., Ntziachristos, P., Aranda-Orgilles, B., Perez-Garcia, A., Shi, J., Vakoc, C., et al. (2013). The ubiquitin ligase FBXW7 modulates leukemia-initiating cell activity by regulating MYC stability. Cell *153*, 1552–1566.

Le, L.Q., and Parada, L.F. (2007). Tumor microenvironment and neurofibromatosis type I: connecting the GAPs. Oncogene *26*, 4609–4616.

Le, L.Q., Shipman, T., Burns, D.K., and Parada, L.F. (2009). Cell of origin and microenvironment contribution for NF1-associated dermal neurofibromas. Cell Stem Cell *4*, 453–463.

Letai, A., Bassik, M.C., Walensky, L.D., Sorcinelli, M.D., Weiler, S., and Korsmeyer, S.J. (2002). Distinct BH3 domains either sensitize or activate mitochondrial apoptosis, serving as prototype cancer therapeutics. Cancer Cell *2*, 183–192.

Ling, B.C., Wu, J., Miller, S.J., Monk, K.R., Shamekh, R., Rizvi, T.A., Decourten-Myers, G., Vogel, K.S., DeClue, J.E., and Ratner, N. (2005). Role for the epidermal growth factor receptor in neurofibromatosis-related peripheral nerve tumorigenesis. Cancer Cell *7*, 65–75.

Lovén, J., Hoke, H.A., Lin, C.Y., Lau, A., Orlando, D.A., Vakoc, C.R., Bradner, J.E., Lee, T.I., and Young, R.A. (2013). Selective inhibition of tumor oncogenes by disruption of super-enhancers. Cell *153*, 320–334.

Martin, G.A., Viskochil, D., Bollag, G., McCabe, P.C., Crosier, W.J., Haubruck, H., Conroy, L., Clark, R., O'Connell, P., Cawthon, R.M., et al. (1990). The GAP-related domain of the neurofibromatosis type 1 gene product interacts with ras p21. Cell *63*, 843–849.

Mo, W., Chen, J., Patel, A., Zhang, L., Chau, V., Li, Y., Cho, W., Lim, K., Xu, J., Lazar, A.J., et al. (2013). CXCR4/CXCL12 mediate autocrine cell- cycle progression in NF1-associated malignant peripheral nerve sheath tumors. Cell *152*, 1077–1090.

Mochizuki, K., Nishiyama, A., Jang, M.K., Dey, A., Ghosh, A., Tamura, T., Natsume, H., Yao, H., and Ozato, K. (2008). The bromodomain protein Brd4 stimulates G1 gene transcription and promotes progression to S phase. J. Biol. Chem. *283*, 9040–9048.

Patel, A.V., Eaves, D., Jessen, W.J., Rizvi, T.A., Ecsedy, J.A., Qian, M.G., Aronow, B.J., Perentesis, J.P., Serra, E., Cripe, T.P., et al. (2012). Ras-driven transcriptome analysis identifies aurora kinase A as a potential malignant peripheral nerve sheath tumor therapeutic target. Clin. Cancer Res. *18*, 5020–5030.

Perrone, F., Da Riva, L., Orsenigo, M., Losa, M., Jocollè, G., Millefanti, C., Pastore, E., Gronchi, A., Pierotti, M.A., and Pilotti, S. (2009). PDGFRA, PDGFRB, EGFR, and downstream signaling activation in malignant peripheral nerve sheath tumor. Neuro-oncol. *11*, 725–736.

Perry, A., Kunz, S.N., Fuller, C.E., Banerjee, R., Marley, E.F., Liapis, H., Watson, M.A., and Gutmann, D.H. (2002). Differential NF1, p16, and EGFR patterns by interphase cytogenetics (FISH) in malignant peripheral nerve sheath tumor (MPNST) and morphologically similar spindle cell neoplasms. J. Neuropathol. Exp. Neurol. *61*, 702–709.

Pietenpol, J.A., and Stewart, Z.A. (2002). Cell cycle checkpoint signaling: cell cycle arrest versus apoptosis. Toxicology *181-182*, 475–481.

Rahrmann, E.P., Watson, A.L., Keng, V.W., Choi, K., Moriarity, B.S., Beckmann, D.A., Wolf, N.K., Sarver, A., Collins, M.H., Moertel, C.L., et al. (2013). Forward genetic screen for malignant peripheral nerve sheath tumor formation identifies new genes and pathways driving tumorigenesis. Nat. Genet. *45*, 756–766.

Shannon, K.M., Watterson, J., Johnson, P., O'Connell, P., Lange, B., Shah, N., Steinherz, P., Kan, Y.W., and Priest, J.R. (1992). Monosomy 7 myeloproliferative disease in children with neurofibromatosis, type 1: epidemiology and molecular analysis. Blood *79*, 1311–1318.

Tait, S.W.G., and Green, D.R. (2010). Mitochondria and cell death: outer membrane permeabilization and beyond. Nat. Rev. Mol. Cell Biol. *11*, 621–632.

Torres, K.E., Zhu, Q.-S., Bill, K., Lopez, G., Ghadimi, M.P., Xie, X., Young, E.D., Liu, J., Nguyen, T., Bolshakov, S., et al. (2011). Activated MET is a molecular prognosticator and potential therapeutic target for malignant peripheral nerve sheath tumors. Clin. Cancer Res. *17*, 3943–3955.

Vogel, K.S., Klesse, L.J., Velasco-Miguel, S., Meyers, K., Rushing, E.J., and Parada, L.F. (1999). Mouse tumor model for neurofibromatosis type 1. Science *286*, 2176–2179.

Wallace, M.R., Marchuk, D.A., Andersen, L.B., Letcher, R., Odeh, H.M., Saulino, A.M., Fountain, J.W., Brereton, A., Nicholson, J., Mitchell, A.L., et al. (1990). Type 1 neurofibromatosis gene: identification of a large transcript disrupted in three NF1 patients. Science *249*, 181–186.

Watson, A.L., Rahrmann, E.P., Moriarity, B.S., Choi, K., Conboy, C.B., Greeley, A.D., Halfond, A.L., Anderson, L.K., Wahl, B.R., Keng, V.W., et al. (2013). Canonical Wnt/β-catenin signaling drives human schwann cell transformation, progression, and tumor maintenance. Cancer Discov. *3*, 674–689.

Wei, M.C., Zong, W.-X., Cheng, E.H.-Y., Lindsten, T., Panoutsakopoulou, V., Ross, A.J., Roth, K.A., MacGregor, G.R., Thompson, C.B., and Korsmeyer, S.J. (2001). Proapoptotic BAX and BAK: a requisite gateway to mitochondrial dysfunction and death. Science *292*, 727–730.

Wu, S.-Y., and Chiang, C.-M. (2007). The double bromodomain-containing chromatin adaptor Brd4 and transcriptional regulation. J. Biol. Chem. *282*, 13141–13145.

Wu, J., Patmore, D.M., Jousma, E., Eaves, D.W., Breving, K., Patel, A.V., Schwartz, E.B., Fuchs, J.R., Cripe, T.P., Stemmer-Rachamimov, A.O., and Ratner, N. (2013a). EGFR-STAT3 signaling promotes formation of malignant peripheral nerve sheath tumors. Oncogene. Published online January 14, 2013. http://dx.doi.org/10.1038/onc.2012.579.

Wu, S.-Y., Lee, A.Y., Lai, H.-T., Zhang, H., and Chiang, C.-M. (2013b). Phospho switch triggers Brd4 chromatin binding and activator recruitment for gene-specific targeting. Mol. Cell *49*, 843–857.

Yang, Z., Yik, J.H.N., Chen, R., He, N., Jang, M.K., Ozato, K., and Zhou, Q. (2005). Recruitment of P-TEFb for stimulation of transcriptional elongation by the bromodomain protein Brd4. Mol. Cell *19*, 535–545.

Yang, Z., He, N., and Zhou, Q. (2008). Brd4 recruits P-TEFb to chromosomes at late mitosis to promote G1 gene expression and cell cycle progression. Mol. Cell. Biol. *28*, 967–976.

Youle, R.J., and Strasser, A. (2008). The BCL-2 protein family: opposing activities that mediate cell death. Nat. Rev. Mol. Cell Biol. *9*, 47–59.

Zou, C., Smith, K.D., Liu, J., Lahat, G., Myers, S., Wang, W.-L., Zhang, W., McCutcheon, I.E., Slopis, J.M., Lazar, A.J., et al. (2009). Clinical, Pathological, and Molecular Variables Predictive of Malignant Peripheral Nerve. Sheath Tumor Outcome. Ann. Surg. *249*, 1014–1022.

Zuber, J., Shi, J., Wang, E., Rappaport, A.R., Herrmann, H., Sison, E.A., Magoon, D., Qi, J., Blatt, K., Wunderlich, M., et al. (2011). RNAi screen identifies Brd4 as a therapeutic target in acute myeloid leukaemia. Nature *478*, 524–528.